THE JOURNAL OF IMMUNOLOGY

Agonist Anti-Human CD27 Monoclonal Antibody Induces T Cell Activation and Tumor Immunity in Human CD27–Transgenic Mice

Li-Zhen He, Naseem Prostak, Lawrence J. Thomas, Laura Vitale, Jeffrey Weidlick, Andrea Crocker, Catherine D. Pilsmaker, Sarah M. Round, Alison Tutt, Martin J. Glennie, Henry Marsh and Tibor Keler

J Immunol published online 11 September 2013
http://www.jimmunol.org/content/early/2013/09/11/jimmunol.1300409

The Journal of Immunology is published twice each month by The American Association of Immunologists, Inc., 9650 Rockville Pike, Bethesda, MD 20814-3994.

Print ISSN: 0022-1767 Online ISSN: 1550-6606.

Published September 11, 2013, doi:10.4049/jimmunol.1300409

Agonist Anti-Human CD27 Monoclonal Antibody Induces T Cell Activation and Tumor Immunity in Human CD27–Transgenic Mice

Li-Zhen He,* Naseem Prostak,*,[1] Lawrence J. Thomas,† Laura Vitale,* Jeffrey Weidlick,* Andrea Crocker,* Catherine D. Pilsmaker,† Sarah M. Round,† Alison Tutt,‡ Martin J. Glennie,‡ Henry Marsh,† and Tibor Keler*

The CD70/CD27 pathway plays a significant role in the control of immunity and tolerance, and previous studies demonstrated that targeting murine CD27 (mCD27) with agonist mAbs can mediate antitumor efficacy. We sought to exploit the potential of this pathway for immunotherapy by developing 1F5, a fully human IgG1 mAb to human CD27 (hCD27) with agonist activity. We developed transgenic mice expressing hCD27 under control of its native promoter for in vivo testing of the Ab. The expression and regulation of hCD27 in hCD27-transgenic (hCD27-Tg) mice were consistent with the understood biology of CD27 in humans. In vitro, 1F5 effectively induced proliferation and cytokine production from hCD27-Tg–derived T cells when combined with TCR stimulation. Administration of 1F5 to hCD27-Tg mice enhanced Ag-specific $CD8^+$ T cell responses to protein vaccination comparably to an agonist anti-mCD27 mAb. In syngeneic mouse tumor models, 1F5 showed potent antitumor efficacy and induction of protective immunity, which was dependent on $CD4^+$ and $CD8^+$ T cells. The requirement of FcR engagement for the agonistic and antitumor activities of 1F5 was demonstrated using an aglycosylated version of the 1F5 mAb. These data with regard to the targeting of hCD27 are consistent with previous reports on targeting mCD27 and provide a rationale for the clinical development of the 1F5 mAb, for which studies in advanced cancer patients have been initiated under the name CDX-1127. ***The Journal of Immunology*****, 2013, 191: 000–000.**

The use of Abs targeting immunoregulatory molecules for the treatment of cancer and other diseases has generated significant interest in recent years (1, 2). In particular, the clinical data from melanoma patients treated with ipilimumab, an Ab that blocks CTLA-4 function, have brought validation to this approach (3). More recent results with Abs that block the checkpoint inhibitory molecule PD1 are adding to the promise of effective and safe treatments for cancers using immunomodulatory approaches (4, 5). There are limited clinical data available with Abs that provide immunoactivation through T cell costimulation. Targeting members of the TNFR superfamily, including CD40, CD134 (OX40), and CD137 (4-1BB), with agonist Abs showed evidence of clinical activity, but it is accompanied by limitations related to toxicity (6–9).

Until recently, CD27, a costimulatory molecule on T cells and a member of the TNFR superfamily, largely has been overlooked as a therapeutic target for immunotherapy. CD27 is a disulphide-linked homodimer of 120 kDa and a type I transmembrane molecule that is constitutively expressed on naive and activated T cells, memory B cells, and a subset of NK cells (10). In this regard, CD27 differs from other members of the TNFR family, which are expressed primarily upon cellular activation (11–13). CD27 is known to play key roles in diverse immunological processes, such as T cell activation, effector function, maturation, and survival, as well as NK cell proliferation and cytotoxicity (14–18). Physiologically, CD27 costimulatory signaling is controlled by the restricted expression of its unique ligand, CD70, which is virtually absent on resting cells but is transiently upregulated on lymphocytes and dendritic cells upon their activation (17, 19, 20).

Several lines of evidence suggest that CD27 costimulation could provide effective T cell–mediated antitumor or antiviral immunity. Early studies showed that engineered expression of CD70 on tumor cells increased their immunogenicity and antitumor activity when transplanted into mice (21, 22). Arens et al. (23) demonstrated that constitutive expression of CD70 on B cells in CD70-transgenic mice increased the Ag-specific T cell response and protected mice from lethal tumor challenge. Studies using CD70–Ig fusion protein demonstrated that CD27 stimulation, in conjunction with protein vaccination, significantly enhanced the magnitude and quality of the $CD8^+$ T cell response (24). In related work, Keller et al. (25) demonstrated that the engineered expression of CD70 on steady-state dendritic cells was sufficient to overcome tolerance and induced potent Ag-specific immunity, and more recent studies (26) showed that CD27 stimulation can lower the threshold of $CD8^+$ T cell activation to low-affinity Ags and provide a broader repertoire of Ag-reactive T cells.

*Celldex Therapeutics, Inc., Phillipsburg, NJ 08865; †Celldex Therapeutics, Inc., Needham, MA 02494; and ‡Antibody and Vaccine Group (MP88), Cancer Sciences Unit, Faculty of Medicine, University of Southampton, Southampton SO16 6YD, United Kingdom

[1]Current address: Eurofins Lancaster Laboratories, Inc., c/o Janssen R&D, LLC, Raritan, NJ.

Received for publication February 11, 2013. Accepted for publication August 8, 2013.

Address correspondence and reprint requests to Dr. Tibor Keler, Celldex Therapeutics, Inc., 222 Cameron Drive, Phillipsburg, NJ 08865. E-mail address: tkeler@celldextherapeutics.com

The online version of this article contains supplemental material.

Abbreviations used in this article: BAC, bacterial artificial chromosome; hCD27, human CD27; hCD27 Tg, human CD27 transgenic; hIgG1, human IgG1; ICS, intracellular cytokine staining; IHC, immunohistochemistry; LN, lymph node; mCD27, murine CD27; MFI, mean fluorescence intensity; PB, peripheral blood; WT, wild-type.

The therapeutic effect of an anti-CD27 agonistic mAb was first shown in studies (27) investigating the mechanisms leading to antitumor responses following treatment with an agonist anti-CD40 mAb. Surprisingly, a CD70 mAb that blocked the CD70/CD27 costimulatory pathway completely abolished the therapeutic effect of anti-CD40 mAb treatment in a BCL1 lymphoma model, demonstrating that CD27 signaling was necessary for the efficacy of anti-CD40 in this tumor model. This led to the development and testing of a rat anti-mouse CD27 mAb, AT124-1, which indeed provided similar antilymphoma efficacy as did the anti-CD40 mAb (27). The antitumor efficacy of CD27 targeting was later reproduced in the EG7 thymoma model by Sakanishi and Yagita (28) using novel anti-mouse CD27 mAbs. These studies were extended by Roberts et al. (29), who demonstrated the T cell–dependent mechanism of anti-CD27 therapy using RAG2- or IFN-γ–knockout mice, which showed minimal or no antitumor activity of the anti-CD27 mAbs in a B16cOVA model.

We developed a fully human Ab, 1F5, which recognizes human CD27 (hCD27) with high affinity, blocks soluble CD70 binding, and inhibits the growth of $CD27^+$ human lymphoma cells in SCID mice (30). In this study, we generated a human CD27-transgenic (hCD27-Tg) mouse model to investigate the agonistic activities of 1F5 and its antitumor efficacy. 1F5 recognized and stimulated hCD27-expressing T cells from the transgenic mice in vitro, enhanced the level of Ag-specific $CD8^+$ T cells in vivo, and mediated potent antitumor immunity. Based partly on these results, the 1F5 mAb recently entered clinical development under the name CDX-1127.

Materials and Methods

Anti-CD27 Abs

A fully human anti-human CD27 Ab 1F5 was generated and characterized as described elsewhere (30). The N297S mutation was introduced into 1F5 by site-directed mutagenesis (Stratagene) and confirmed by DNA sequencing. FreeStyle CHO-S cells (Invitrogen) were transiently transfected to express the $1F5_{N297S}$ mutant Ab, which was subsequently purified from culture supernatants with a MabSelect SuRe Pro A column (GE Healthcare). The rat anti–murine CD27 (mCD27) mAb AT124-1 was described previously (27). The endotoxin level for all Abs used in functional assays or in vivo studies was <1.0 EU/mg, as measured by the Gel Clot LAL method (Lonza).

Biacore analysis

Binding affinity and binding kinetics of the 1F5 and $1F5_{N297S}$ mutant Abs to mouse FcγRs were examined by surface plasmon resonance analysis using a Biacore 2000 SPR instrument (Biacore, Uppsala, Sweden), according to the manufacturer's guidelines. The Abs 1F5 and $1F5_{N297S}$ were covalently linked to a Biacore CM5 sensor chip using standard amine coupling chemistry with an Amine Coupling Kit (Biacore). The Mouse FcγRs (R&D Systems) were allowed to flow over the sensor chip at concentrations ranging from 12.5 to 400 nM and at a flow rate of 30 μl/min for 300 s. A blank flow cell with no protein immobilized was used for background subtraction. The affinity and kinetic parameters were derived from the time-dependent association and dissociation curves using BIAevaluation software (Biacore).

Generation of hCD27-Tg mice

A human bacterial artificial chromosome (BAC) clone was identified and shown to contain the entire CD27 gene and promoter by PCR and sequencing analysis. A 175-kb insert DNA was prepared from the BAC and microinjected into fertilized oocytes, which were transplanted into the C57BL/6-SJL hybrid strain. The transgene transcript was detected by RT-PCR with hCD27-specific primers in total RNA extracted from peripheral blood (PB) leukocytes of three founder mice. Two transgenic lines with very similar expression profiles were established, and one line was backcrossed to C57BL/6, BALB/c, and C3H genetic backgrounds for more than five generations using selected breeders based on congenic analysis (IDEXX RADIL). All mice were housed under specific pathogen–free conditions in the Celldex animal facilities and were used in accordance with the guidelines established by the Institutional Animal Care and Use Committees at our institution.

Characterization of hCD27-Tg mice

Immunohistochemistry (IHC) and flow cytometry were performed to examine the expression profile of the hCD27 transgene. Sixteen organs (skin, lymph nodes [LNs], thymus, spleen, liver, brain, pituitary, heart, lung, kidney, jejunum, ileum, colon, testis/ovary, and muscle) were collected from C57BL/6 hCD27-Tg homozygous and heterozygous mice and wild-type (WT) littermates. Frozen sections were cut and stained with one of our well-characterized human anti-hCD27 mAbs, human IgG1 (hIgG1) clone 3H8; with murine IgG1 clone L128 (BD Biosciences) for hCD27; or with either hamster IgG1 clone LG3A10 (BD Biosciences) or rat IgG2a clone 137910 (R&D Systems) for mCD27. All of the primary Abs and their isotype controls were conjugated to FITC. Sections were then stained with rabbit anti-FITC Ab (Invitrogen), detected using the Dako EnVision Kit, and counterstained with hematoxylin.

Flow cytometry was performed on single-cell suspensions prepared from PB, LNs, spleen, and thymus of hCD27-Tg homozygous and heterozygous mice and their WT littermates by manual mechanical dissociation, followed by lysis of RBCs. After blocking non-Ag–specific staining with anti-CD16/CD32 mAb clone 2.4G2, cells were stained with anti-CD27 Abs and for lymphocyte surface markers, including CD3ε, CD4, CD8a, CD19, and NK1.1 (BD Biosciences). Isotype controls for all Abs were included. Analyses were done on an LSR or FACSCanto II flow cytometer (BD Immunocytometry Systems).

We used ELISA to compare the binding of hCD27 and mCD27 with recombinant murine CD70. Briefly, CD70 (R&D Systems) was coated on a plate at 2 μg/ml, and then the plates were blocked with 5% albumin in PBS solution. Dilutions of hCD27-Fc, mCD27-Fc, and negative control human TIM-1–Fc (all from R&D Systems) were added at various concentrations in duplicate, and binding was detected with HRP-labeled goat anti-human IgG Fc. The absorbance at 450 nm was determined using a microplate reader.

Regulation of CD27 expression

For T cell activation, microtiter wells were precoated with anti-CD3ε (145-2C11) at 5 μg/ml or received soluble murine IL-2 (both from R&D Systems) at 100 ng/ml or the mitogen PHA at 5 μg/ml final concentration. Splenocytes from hCD27-Tg homozygous and WT mice were incubated in the plate for 3 d and then stained for hCD27 or mCD27 and the surface markers CD3, CD4, and CD8. The mean fluorescence intensity (MFI) for CD27 was compared for $CD4^+$- or $CD8^+$-gated cells. The culture supernatants were collected to measure soluble hCD27 and mCD27 levels by sandwich ELISA using anti-human or anti-murine Ab pairs and standards from Sanquin and R&D Systems.

T cell proliferation and intracellular cytokine staining

T cells were isolated by depletion of non-T cells from splenocytes of homozygous C57BL/6 hCD27-Tg mice using the *Pan* T Cell Isolation Kit II (Miltenyi Biotec) and labeled with 2.5 μM CFSE (Invitrogen). T cells (0.5×10^6 /well) were transferred to 96-well U-bottom plates that had been precoated or not with 2 μg/ml CD3ε mAb 145-2C11. 1F5 or an irrelevant hIgG1 was added to the cultures at a final concentration of 0.2 μg/ml in the presence or absence of 10-fold excess of murine anti-human IgG (Jackson ImmunoResearch Lab) for cross-linking. Immobilized CD3ε mAb, with or without 10 μg/ml coated recombinant mouse CD70, was also included for reference. The cultures were kept at 37°C in an incubator for 3 d, and brefeldin A (Sigma-Aldrich) was added to a final concentration of 10 μg/ml for the last 4 h. Cells were stained with blue fluorescent reactive dye (Live/Dead Fixable Dead Cell Stain Kit; Invitrogen), surface CD8, CD4, and human CD27 (clone MT271; BD Biosciences, noncompetitive with 1F5 binding), and, subsequently for intracellular IFN-γ and TNF-α after fixing and permeabilizing with Cytofix/Cytoperm (BD Biosciences). Samples were analyzed using a FACSCanto II flow cytometer.

Immunization and Ag-specific T cell response

C57BL/6 hCD27-Tg and WT littermates were dosed i.v. with 5 mg chicken OVA (Sigma-Aldrich) and 250 μg 1F5, rat anti-murine CD27 (clone AT124-1), or isotype control on day 0, with an additional 250 μg Ab the next day. In subsequent studies, we used i.p. dosing of OVA (5 mg) and a single dose of 1F5 or $1F5_{N297S}$ (50 μg) on day 0. Splenocytes were collected on day 7 for tetramer staining, IFN-γ intracellular cytokine staining (ICS), and ELISPOT assays following RBC lysis. Splenocytes (1×10^6) were stained with 10 μl H-$2K^b$-SIINFEKL tetramer (Beckman Coulter) in conjunction with surface CD8 and IFN-γ ICS, as described above. A total of 100,000 events was acquired using an LSR flow cytometer, and the fraction of $tetramer^+$ and IFN-γ^+ cells in the $CD8^+$-gated population was determined. For ELISPOT, assays were carried out by incubating 0.25×10^6 or 1.0×10^6 splenocytes/well in triplicate in IFN-γ

Ab–coated 96-well filtration plates overnight in the presence or absence of 2 μg/ml SIINFEKL peptide. Spots were developed using an IFN-γ Ab reagent set with AEC substrate chromagen (BD Biosciences) and counted by ZellNet Consulting.

Tumor-challenge studies

The antitumor activity of 1F5 was assessed in four syngeneic mouse tumor models. B-lymphoma BCL1 was maintained and expanded in WT BALB/c mice. For the BCL1 tumor model, ~10^7 splenocytes from the in vivo expansion were administered i.v. to the BALB/c hCD27-Tg mice. The colon carcinoma CT26 (American Type Culture Collection) was cultured in RPMI 1640 with 10% FBS. For this tumor model, 10^4 CT26 cells were administered s.c. to BALB/c hCD27-Tg mice. The thymoma EL4 and its OVA-expressing derivative EG7 (both from American Type Culture Collection) were grown in RPMI 1640/10% FBS and in the presence of 0.5 mg/ml G418 for EG7 cells. For the tumor model, 0.5×10^6 EL4 cells or 1.0×10^6 EG7 cells were administered s.c. to C57BL/6 hCD27-Tg mice. 1F5 Ab was administered over a dose range of 2 to 600 μg as multiple i.p. injections, as indicated in the figure legends. Control cohorts included hCD27-Tg mice injected with saline or hIgG1 and WT mice injected with 1F5. Mice were observed daily, and tumor size was measured at least twice a week with calipers. Tumor volume was calculated using a modified ellipsoid formula (length × width^2 ÷ 2). Mice were euthanized when they met predetermined end points approved by the Institutional Animal Care and Use Committee. Secondary tumor challenge was performed in mice free of measurable tumors ~3 mo postprimary tumor inoculation and paired with the same number of control naive mice. No further treatment was administered.

T cell–depletion studies were performed using anti-CD4 (GK1.5) or anti-CD8 (53-6.7; both from eBioscience) Abs to deplete $CD4^+$ and $CD8^+$ T cells, respectively. In the CT26 model, depleting Abs were administered i.p. on day 1 (500 μg) and day 10 (50 μg) posttumor inoculation. In the EG7 model, depleting Abs were administered i.p. on day 3 (500 μg) and day 12 (100 μg). In pilot studies, these regimens were shown to effectively deplete $CD4^+$ or $CD8^+$ splenic T cells by flow cytometry.

Statistical analysis

The Student *t* test was used for mean ± SD (two-tailed unequal variance) comparisons. Kaplan–Meier analysis was used for survival.

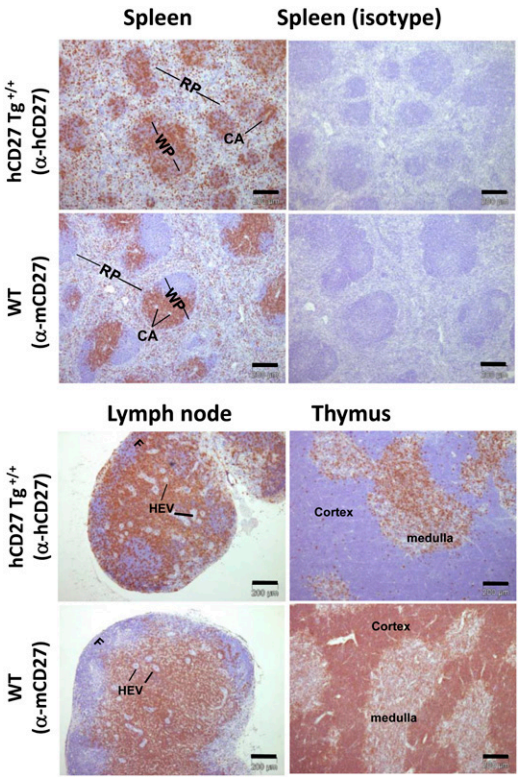

FIGURE 1. Tissue expression of hCD27 in hCD27-Tg mice. Immunostaining of lymphoid tissue from C57BL/6 hCD27-Tg and C57BL/6 WT mice with anti-hCD27 mAb L128-FITC and its isotype control (0.1 μg/ml) or anti-mCD27 mAb LG3A10-FITC and its isotype control (0.5 μg/ml) on acetone-fixed, frozen tissue sections. The sections were counterstained with Mayer's hematoxylin. Scale bars, 200 μm. CA, Central artery; HEV, high endothelial venule; RP, red pulp; WP, white pulp.

Results

Development and characterization of hCD27-Tg mice

hCD27-Tg mice were generated by standard microinjection techniques in the C57BL/6-SJL hybrid strain using a 175-kb fragment of BAC DNA including the entire CD27 gene and additional upstream sequences. Therefore, expression of the hCD27 transgene was anticipated to be controlled by its own promoter. One of three founder mice was expanded and successfully back-crossed onto the C57BL/6, C3H, or BALB/c background. Characterization of the transgene expression was performed by IHC on 16 tissues collected from hCD27-Tg and WT mice using human and mouse-specific anti-CD27 Abs. Limited expression of hCD27 or mCD27 was observed in nonlymphatic tissues that appear to be scattered infiltrating lymphocytes or lymphatic structures (data not shown). As expected, there was significant staining of CD27 in lymphoid tissues (Fig. 1). IHC staining of hCD27 and mCD27 displayed a generally similar pattern of expression in most lymphoid tissues. In particular, strong staining of hCD27 and mCD27 was observed in T cell areas, such as the periarterial lymphatic sheath in the white pulp of spleen and paracortex of LN, and occasional to rare staining was noted in B cell areas, sinuses, medulla, and red pulp (Fig. 1). We observed a marked difference in the staining pattern for hCD27 compared with the endogenous mCD27 in the thymus, where $hCD27^+$ cells were frequent in medulla but rarely seen in the cortex, whereas mCD27-stained cells were frequent in both medulla and cortex (Fig. 1). This difference is consistent with the previous data on thymic T cells that support a more limited expression of hCD27 compared with mCD27 (31).

Flow cytometry analysis of CD27 expression was performed on cells isolated from PB, LNs, spleen, and thymus of hCD27-Tg mice and WT mice. The frequency of hCD27 and mCD27 expression was observed in a similar percentage of $CD4^+$ (82% versus 86%) and $CD8^+$ (73% versus 85%) T cells from spleen (Fig. 2A). However, there appeared to be a greater variability in the expression level of hCD27, which contained both $CD27^{bright}$ and $CD27^{low}$ populations, compared with mCD27, which was more homogeneous with $CD27^{intermediate}$ staining. hCD27 was expressed at a higher frequency than was mCD27 on $CD19^+$ B cells (10% versus 2%), which likely represents the difference in CD27 expression on somatically mutated memory B cells between the two species (32). hCD27 and endogenous mCD27 were predominantly coexpressed in lymphoid tissues (Fig. 2B) with some $hCD27^+/mCD27^-$ and $hCD27^-/mCD27^+$ cells observed, which likely represent B cells and NK cells, respectively. hCD27 was expressed at much lower frequency on murine NK cells compared with mCD27 (Fig. 2C).

To evaluate the regulation of hCD27 expression, we investigated the effect of agents that activate T cells and are known to upregulate CD27 expression and shedding (11, 19). PHA or TCR stimulation (anti-CD3ε) upregulated hCD27 and mCD27 expression levels on T cells, as shown by flow cytometry analysis (Fig. 3A). IL-2, as expected, did not enhance hCD27 expression (Fig. 3A). A similar pattern was observed for the shedding of soluble CD27 into the media (Fig. 3B) of the same cultures used for flow cytometry.

Finally, we demonstrated that human CD27 can bind efficiently to murine CD70, which would allow for interactions with its ligand in hCD27-Tg mice (Fig. 4). Overall, the data support that the hCD27 transgene is expressed and regulated in a manner generally

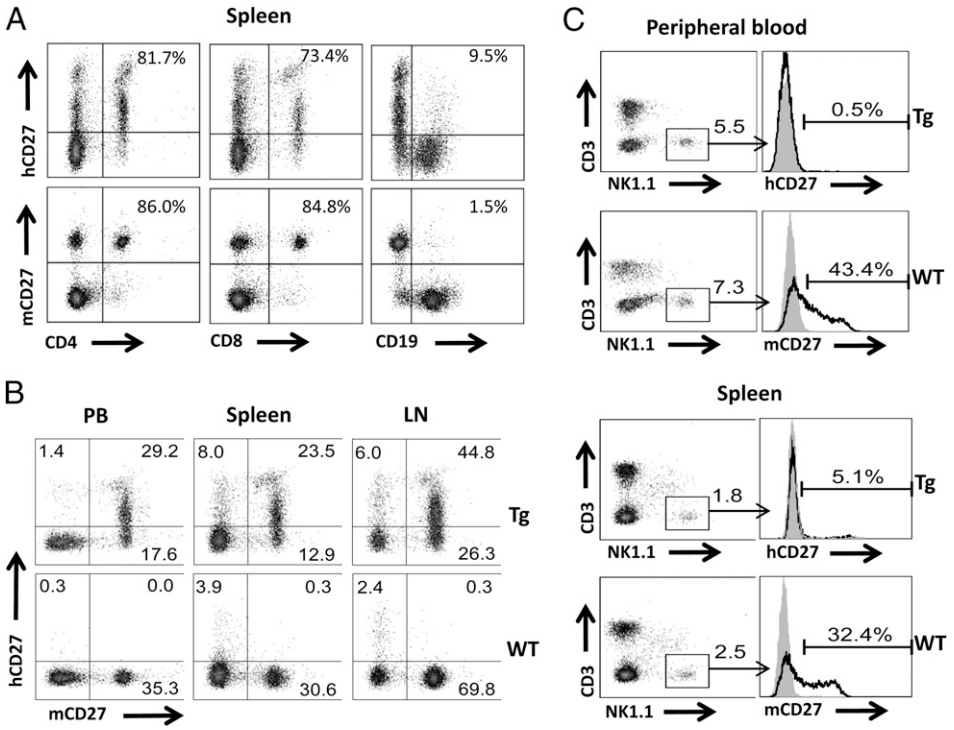

FIGURE 2. Surface expression of hCD27 on cells from hCD27-Tg mice. Organs were harvested from C57BL/6 hCD27-Tg or WT C57BL/6 mice and prepared as single-cell suspensions for staining and analysis by flow cytometry. Representative plots are presented. (**A**) Expression of hCD27 and mCD27 on gated splenic T and B cells. (**B**) Overlapping expression of hCD27 and mCD27 in lymphoid organs from hCD27-Tg mice. (**C**) Lack of significant expression of hCD27 on NK cells in blood or spleen (as defined by $CD3^{-}NK1.1^{+}$).

consistent with the known biology of hCD27, and hCD27-Tg mice would be a useful model for evaluating hCD27-targeting agents.

1F5 triggers proliferation and activation of hCD27-Tg T cells

Proliferation and cytokine-induction experiments were performed on purified T cells from hCD27-Tg mice to demonstrate the functionality of the hCD27 transgene and to confirm the agonist activity of the anti-CD27 mAb 1F5. CD27 costimulation of T cell proliferation requires additional signals, in particular TCR activation (11, 14), and our prior studies using purified T cells from healthy donors confirmed that 1F5 activated human T cells only in the context of TCR stimulation (30). Therefore, CD27 activation was assessed on T cells derived from hCD27-Tg mouse spleens in combination with immobilized anti-CD3ε mAb. As shown in Fig. 5A, the 1F5 mAb combined with a suboptimal stimulation of anti-CD3ε mAb, significantly enhanced $CD8^{+}$ T cell proliferation and IFN-γ production but only when the 1F5 was cross-linked with anti-human IgG. The cross-linked 1F5 also induced the prolifer-

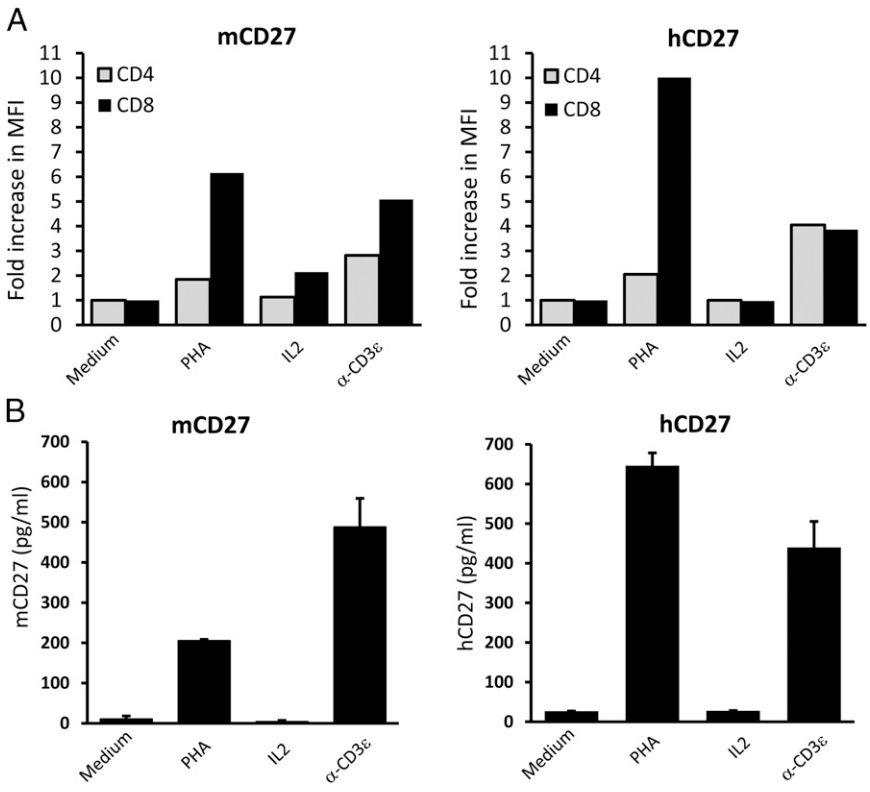

FIGURE 3. Regulation of hCD27 expression in hCD27-Tg mice. Splenocytes from C57BL/6 hCD27-Tg mice were activated for 72 h in wells that were precoated with anti-CD3ε or were exposed to PHA or IL-2 in solution. (**A**) Flow cytometric analysis was performed for hCD27 or mCD27 expression on gated $CD4^{+}$ or $CD8^{+}$ cells. Fold increase in MFI was calculated by comparison with the MFI of the same cells cultured in media without T cell stimulus. (**B**) Supernatants collected at 72 h were tested by hCD27- or mCD27-specific ELISAs and quantified from a standard curve using recombinant hCD27 and mCD27, respectively. Data are representative of three independent experiments.

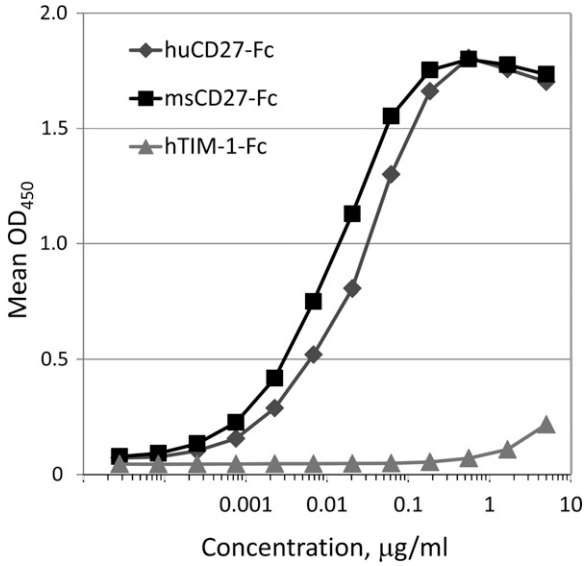

FIGURE 4. hCD27 binds to murine CD70. Microtiter plates coated with recombinant mouse CD70 were incubated with various concentration of hCD27-Fc, mCD27-Fc, or an irrelevant chimeric protein, human TIM-1–Fc. Binding was detected with HRP-labeled goat anti-human IgG Fc, and the average of duplicates was plotted.

ation and cytokine production of $CD4^+$ T cells when combined with anti-CD3ε but to a significantly lower magnitude than that of the $CD8^+$ T cells. We observed the same results for TNF-α production (data not shown). Demonstrating relevance to the activity of the native ligand, we observed a similar effect on $CD8^+$ T cell proliferation and cytokine production with plate-bound murine CD70 combined with anti-CD3ε (Fig. 5B).

1F5 enhances Ag-specific CD8 T cell response

Costimulation of CD27 was shown to effectively enhance $CD8^+$ T cell responses to vaccination using a sCD70–Ig fusion protein (24), which suggests that agonist anti-CD27 mAbs may have similar effects. We compared the ability of 1F5 and rat anti-mCD27 mAb (clone AT124-1) to enhance $CD8^+$ T cell responses to OVA (Fig. 6). The hCD27-Tg mice and WT littermates were immunized with OVA protein and administered two doses of anti-CD27 mAbs or isotype control prior to analysis for OVA-specific $CD8^+$ T cells with H-$2K^b$/SIINFEKL tetramer and IFN-γ ICS (Fig. 6A–C) or by IFN-γ ELISPOT after stimulation with the SIINFEKL peptide (Fig. 6D). The 1F5 mAb and AT124-1 mAb showed a significant enhancement in the percentage and absolute amount of Ag-specific $CD8^+$ T cell responses in hCD27-Tg mice and WT mice, respectively. The activation of the tetramer-stained cells was confirmed by intracellular staining for INF-γ. The specificity of the enhanced response was demonstrated by the weak $CD8^+$ T cell response in WT mice treated with 1F5 or the hCD27-Tg mice treated with an irrelevant hIgG1.

Dose-dependent antitumor activity of 1F5

To assess whether the immunomodulatory activities of 1F5 can be translated to effective antitumor therapy, we investigated the effect of varying doses of 1F5 in the BCL1 tumor model using syngeneic

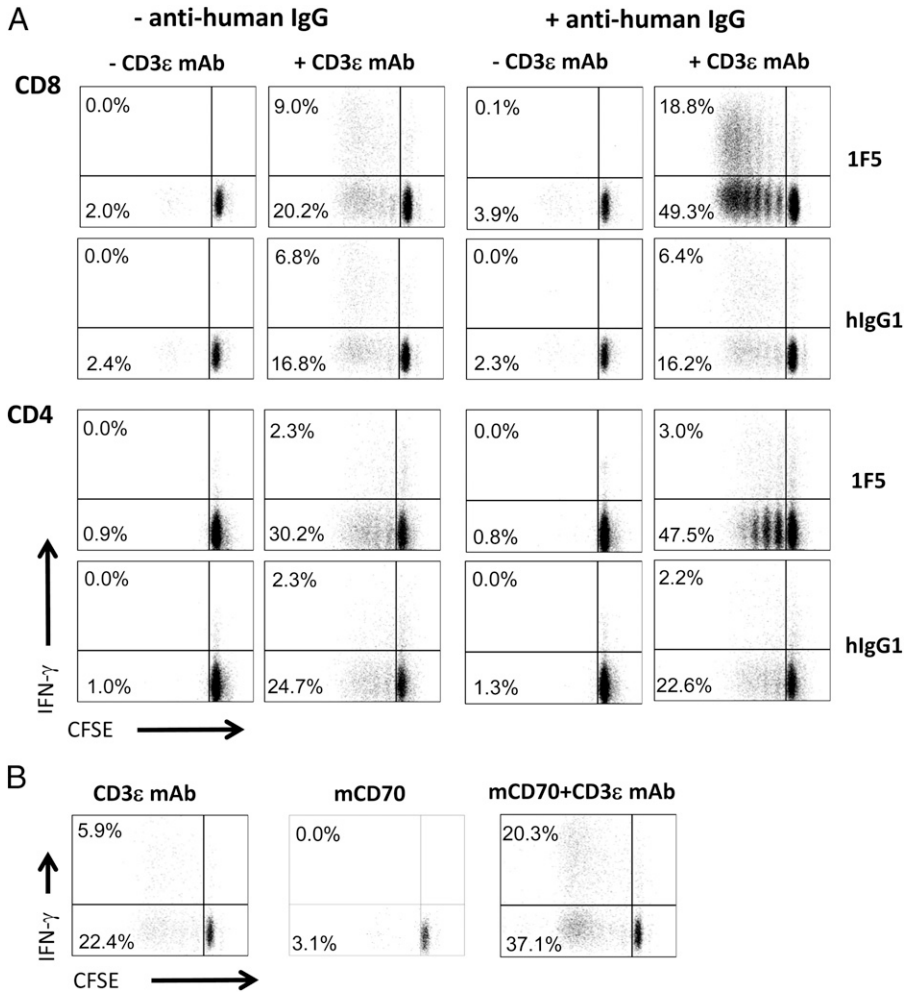

FIGURE 5. Induction of T cell activation and proliferation with 1F5 in vitro. T cells were isolated from spleens of C57BL/6 hCD27-Tg mice by negative selection with MicroBeads, labeled with CFSE, and added to uncoated wells or wells precoated with anti-CD3ε. (**A**) A total of 0.2 μg/ml 1F5 or hIgG1 isotype control, with or without 2 μg/ml mouse anti-human IgG, was added as indicated. After 3 d of incubation, the level of CFSE dilution and intracellular IFN-γ were measured by flow cytometry after gating on $CD8^+$ or $CD4^+$ cells. (**B**) Wells were precoated with anti-CD3ε, mouse CD70, or both and incubated as in (A). The results on gated $CD8^+$ cells are shown. One representative example of two experiments is shown.

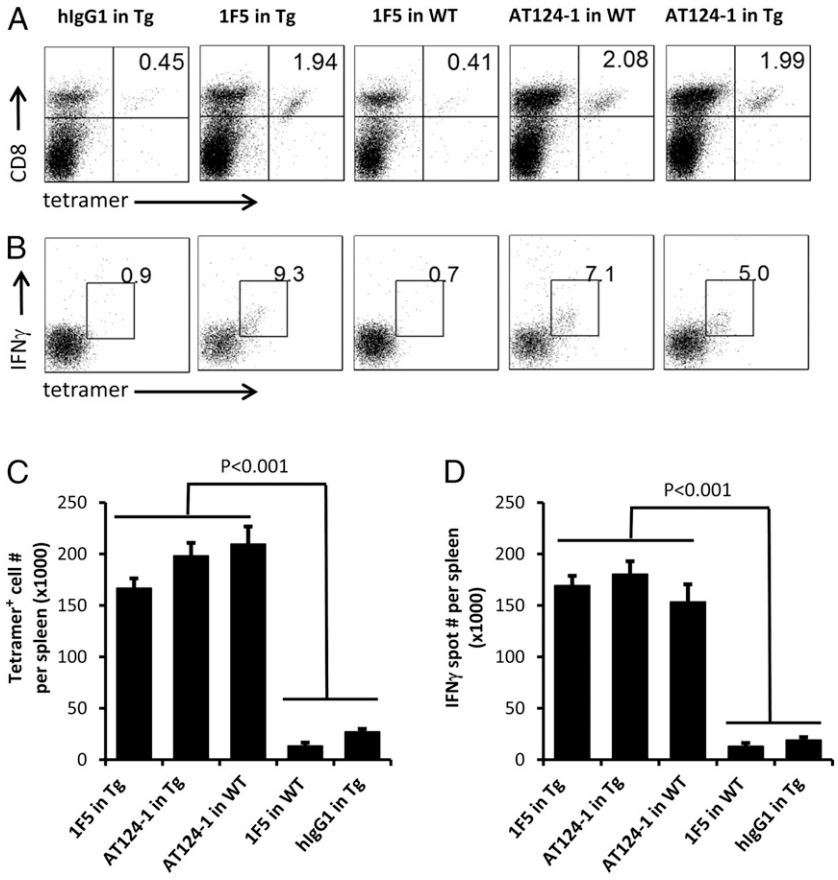

FIGURE 6. 1F5 enhances CD8 response to protein immunization. Human CD27-Tg or WT C57BL/6 mice were injected i.v. with 5 mg of OVA protein and i.p. with 0.25 mg of anti-mCD27 (AT124-1) or anti-hCD27 (1F5) mAb. A second dose of CD27 mAbs (0.25 mg) was administered the next day. Seven days later, the splenocytes were harvested for analysis by flow cytometry and ELISPOT. (**A**) Representative plots of H-2K^b/SIINFEKL tetramer and CD8 staining for each condition. (**B**) Representative plots of tetramer versus IFN-γ intracellular staining in CD8$^+$-gated cells for each condition. (**C**) Mean ± SD of total tetramer$^+$ cells/spleen from three mice/condition. (**D**) IFN-γ ELISPOT assays were performed by overnight stimulation or not with the SIINFEKL peptide. Data are mean ± SD of total SIINFEKL peptide–specific spot numbers/spleen of six mice/condition pooled from three independent experiments.

BALB/c hCD27-Tg mice. We observed significant prolongation of survival in 1F5-treated animals compared with isotype-treated controls when doses ≥ 10 μg were delivered on days 3, 5, 7, 9, and 11 after tumor challenge. The lowest dose of 1F5 tested, five doses of 2 μg, had no survival benefit compared with controls (Fig. 7). There was a trend toward longer median survival times with higher doses of 1F5, although doses of 50, 150, or 600 μg were not statistically different from each other. The 600-μg dose group was statistically significantly different from the 10-μg dose group (median survival of 78 d versus 59 d, respectively, $p = 0.032$). As an additional control, we administered the BCL1 tumor to six WT BALB/c mice, followed by treatment with 1F5 (five doses of 600 μg each using the same schedule as above), but it had no benefit on median survival (23 d), and no mice survived past day 30 (data not shown).

1F5 induces tumor regression and long-term immunity

We further tested the efficacy of the 1F5 mAb in the s.c. implanted colon carcinoma CT26 tumor model, which allowed for tumor growth to be monitored. Groups of BALB/c hCD27-Tg mice were inoculated with CT26 cells and then treated with saline or 1F5 (5 doses of 600 μg on days 3, 5, 7, 9 and 11 posttumor challenge). Initially, tumors grew similarly in both groups of mice; however, in most animals treated with 1F5 this growth was followed by a slowing and subsequent regression of the tumor, which was not observed in the saline-treated mice (Fig. 8A). Mice treated with 1F5 that underwent tumor regression remained tumor free for 3 mo and were rechallenged with CT26 cells (Fig. 8B). All rechallenged mice were resistant to CT26 tumor growth, whereas a concurrent group of similarly challenged naive mice showed rapid tumor

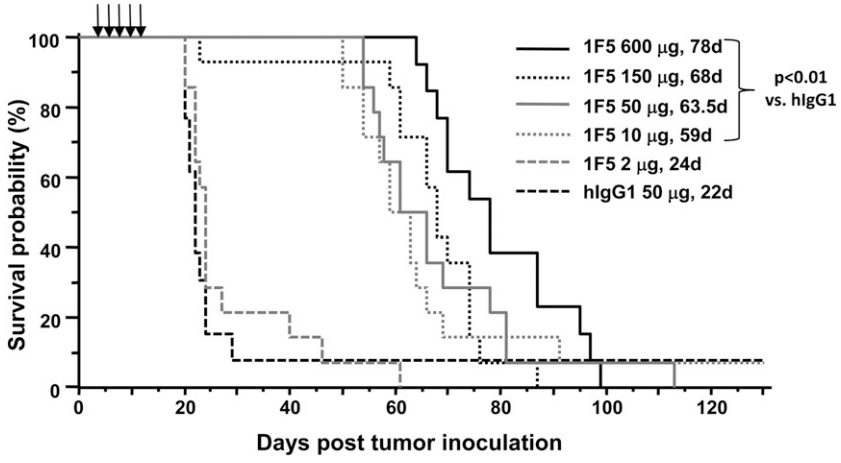

FIGURE 7. Dose-dependent antitumor efficacy of 1F5 in syngeneic BCL1 lymphoma model. Groups of six or seven hCD27-Tg or WT BALB/c mice were inoculated i.v. with 1×10^7 BCL1 cells on day 0. The 1F5 mAb or control hIgG1 was administered i.p. on days 3, 5, 7, 9, and 11 (indicated by arrows) at the indicated doses (μg/injection). Median survival (d) is indicated beside the dose level in the key. Kaplan–Meier survival curves are derived from pooled data of two independent experiments.

progression from the CT26 inoculation. The pattern of tumor regression and immunity to rechallenge indicates the induction of T cell–mediated antitumor and memory responses. When 1F5 administration was delayed until tumors were of significant size (0.15–0.2 cm^3), the treatment effect was diminished, but it still resulted in a measurable survival benefit (Fig. 8C).

The aggressively growing EL4 thymoma was resistant to 1F5 treatment, even when administered early after tumor challenge (Fig. 9A). However, 1F5 induced marked tumor regression in ~40% of mice given EG7 tumors, an OVA-expressing variant of EL4 (Fig. 9B), which suggested the OVA may be the dominant tumor-rejection Ag. Subsequently, we investigated whether mice that rejected EG7 tumors after 1F5 treatment were resistant to either EL4 or EG7 rechallenge (Fig. 9C). The EG7 survivors were protected against EG7 rechallenge, with 90% of the mice never developing tumors. The protection of EG7 survivors against EL4 tumor was substantially lower, but it did result in a clear survival benefit, suggesting that some of the immune response was directed to shared Ags and not only to OVA.

T cell depletion abrogates 1F5 antitumor activity

The contribution of $CD4^+$ and $CD8^+$ T cells to the antitumor activity of 1F5 was investigated by specific depletion of these

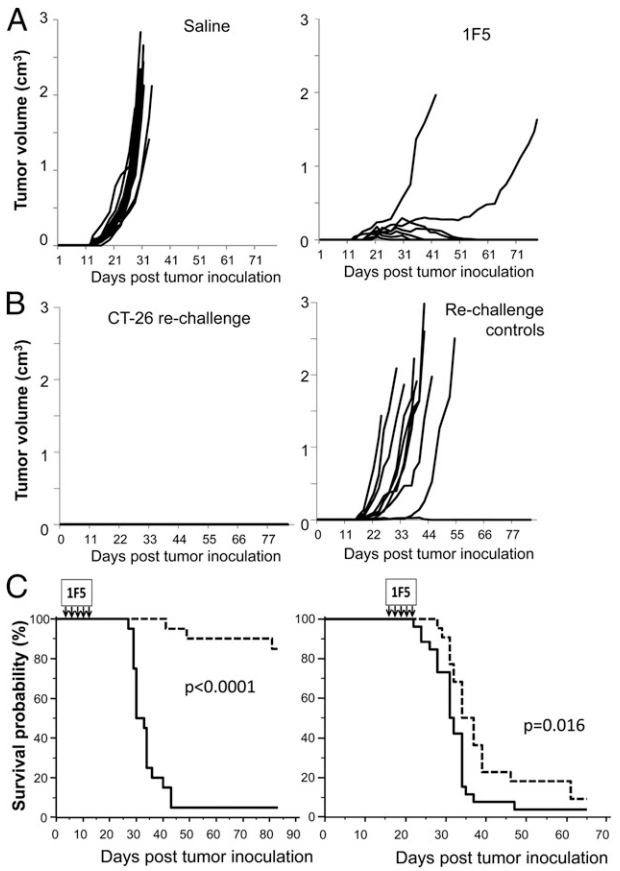

FIGURE 8. Tumor regression and induction of immunity with 1F5 in CT26 colorectal cancer model. (**A**) Groups of 10 hCD27-Tg BALB/c mice were inoculated s.c. with 1×10^4 CT26 cells on day 0. 1F5 (600 μg) or saline was administered i.p. on days 3, 5, 7, 9, and 11, and mice were followed for tumor growth. (**B**) Eight mice surviving the initial tumor challenge after 1F5 treatment were rechallenged with 1×10^4 CT26 cells on day 99. Ten naive mice were challenged at the same time as controls. (**C**) Kaplan–Meier survival curves of animals challenged with 1×10^4 CT26 and treated with 1F5 (600 μg) on days 3, 5, 7, 9, and 11 or on days 15, 17, 19, 21, and 23 (as indicated by arrows). The *p* values shown are relative to saline-treated controls. The data are representative of two independent experiments.

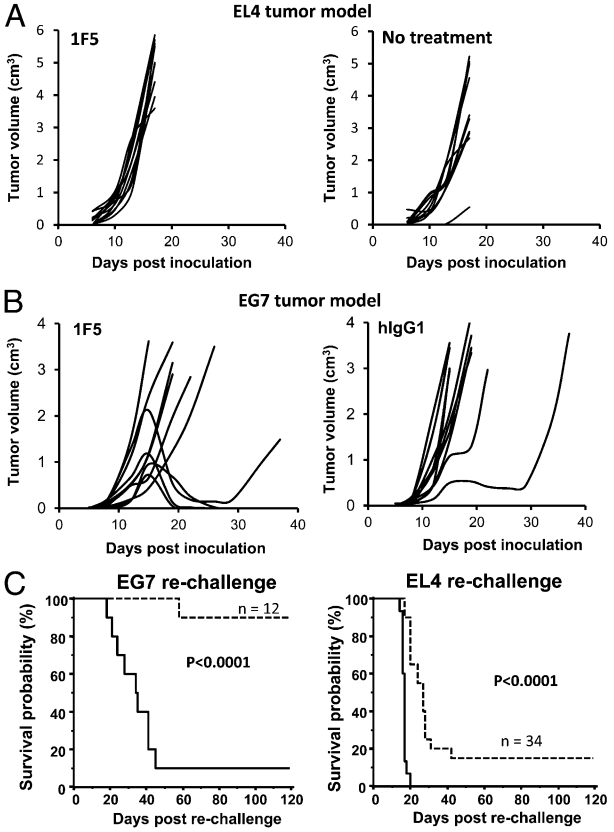

FIGURE 9. Effect of 1F5 in EL4 and EG7 thymoma models. (**A**) Groups of 10 hCD27-Tg C57BL/6 mice were inoculated s.c. with 0.5×10^6 EL4 cells on day 0 and left untreated or received 1F5 (50 μg) on days 5, 8, 11, 14, 17, and 20. (**B**) Groups of 10 hCD27-Tg C57BL/6 mice were inoculated s.c. with 1×10^6 EG7 cells on day 0 and received 1F5 or hIgG1 (50 μg) on days 5, 8, 12, 15, 19, and 22. (**C**) Kaplan–Meier survival curves from pooled data of groups of animals that survived the initial EG7 challenge (dashed lines) and were rechallenged with 10^6 EG7 cells or 0.5×10^6 EL4 cells. Naive animals (solid lines) with the same tumor inoculations were used as controls. The *p* values shown are for rechallenge and naive groups.

populations in the CT26 and EG7 tumor models. Elimination of either $CD4^+$ or $CD8^+$ T cells abolished the enhanced survival benefit from 1F5 in both tumor models (Fig. 10). These results

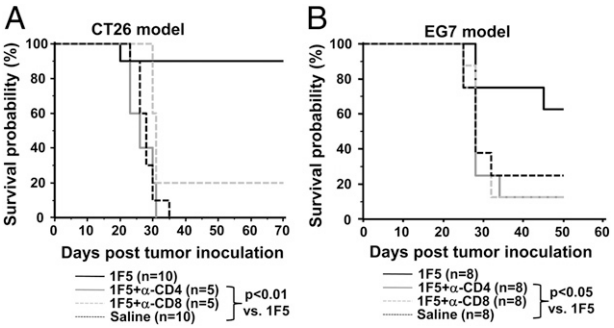

FIGURE 10. 1F5-induced tumor immunity requires both CD4 and CD8 T cells. (**A**) Kaplan–Meier survival curves of hCD27-Tg BALB/c mice inoculated s.c. with 1.5×10^4 CT26 cells on day 0. Animals were treated with 1F5 (600 μg) administered i.p. on days 3, 5, 7, 9, and 11 or with 1F5 combined with either CD4 or CD8 T cell–depleting Abs. Control animals received saline only. (**B**) Kaplan–Meier survival curves of hCD27-Tg C57BL/6 mice inoculated s.c. with 5×10^5 EG7 cells on day 0. Animals were treated with 1F5 (100 μg) administered i.p. on days 5, 8, 11, 14, 17, and 20 alone or combined with either CD4 or CD8 T cell–depleting Abs. Control animals received saline only. Data are representative of two individual experiments.

support the expectation that 1F5 treatment leads to an effective CD8 antitumor response, but they also demonstrate the critical role for $CD4^+$ T cells in this process.

FcR interaction is required for 1F5 activity in vivo

The in vitro studies demonstrated that T cell activation by 1F5 required cross-linking of the Ab. We presumed that this was also required in vivo and likely occurred through interaction with FcγR. To confirm this hypothesis, we introduced a mutation into the 1F5 Fc domain ($1F5_{N297S}$) that resulted in the loss of binding to FcRs (Fig. 11B), as expected (33), but retained the same binding to hCD27 (Fig. 11A). The $1F5_{N297S}$ mutant lost the capacity to enhance the SIINFEKL-specific T cell response when coinjected with OVA protein (Fig. 11C) and was unable to mediate antitumor activity (Fig. 11D). Therefore, we conclude that FcγR engagement is required for the in vivo costimulatory and antitumor activity of 1F5.

Discussion

Targeting the CD27-costimulation pathway with specific Abs showed considerable promise in a variety of murine model systems (27–29) and motivated the development of human anti-hCD27 Abs with the potential for human clinical use. We recently reported on the characterization of the anti-hCD27 mAb 1F5, which was selected based on its effective costimulation of human T cells and potent antitumor activity against CD27-expressing lymphoblastic tumors in immunodeficient (SCID) mice (30). The objective of this study was to establish the costimulatory and antitumor activity of the 1F5 mAb in immunocompetent mice, as well as to investigate the mechanism of 1F5-induced CD27 signaling.

For our in vivo model we generated and characterized hCD27-Tg mice. The expression pattern for the transgene was examined by IHC and flow cytometry on relevant tissues and showed a profile consistent with the endogenous mCD27 and with the expected distribution for hCD27 (11–13). Some discrepancies between murine and human CD27 expression were noted (e.g., broader expression of mCD27 in thymus, higher expression of hCD27 on B cells), which are consistent with the reported literature for CD27 expression in the two species (11, 19). We demonstrated in vitro that the cell surface levels and shedding of hCD27 were appropriately upregulated by PHA and TCR stimulation of spleen-derived T cells. Last, we showed that cross-linking hCD27 with 1F5 in combination with TCR stimulation led to the proliferation and activation (Th1 cytokine production) of hCD27-Tg T cells.

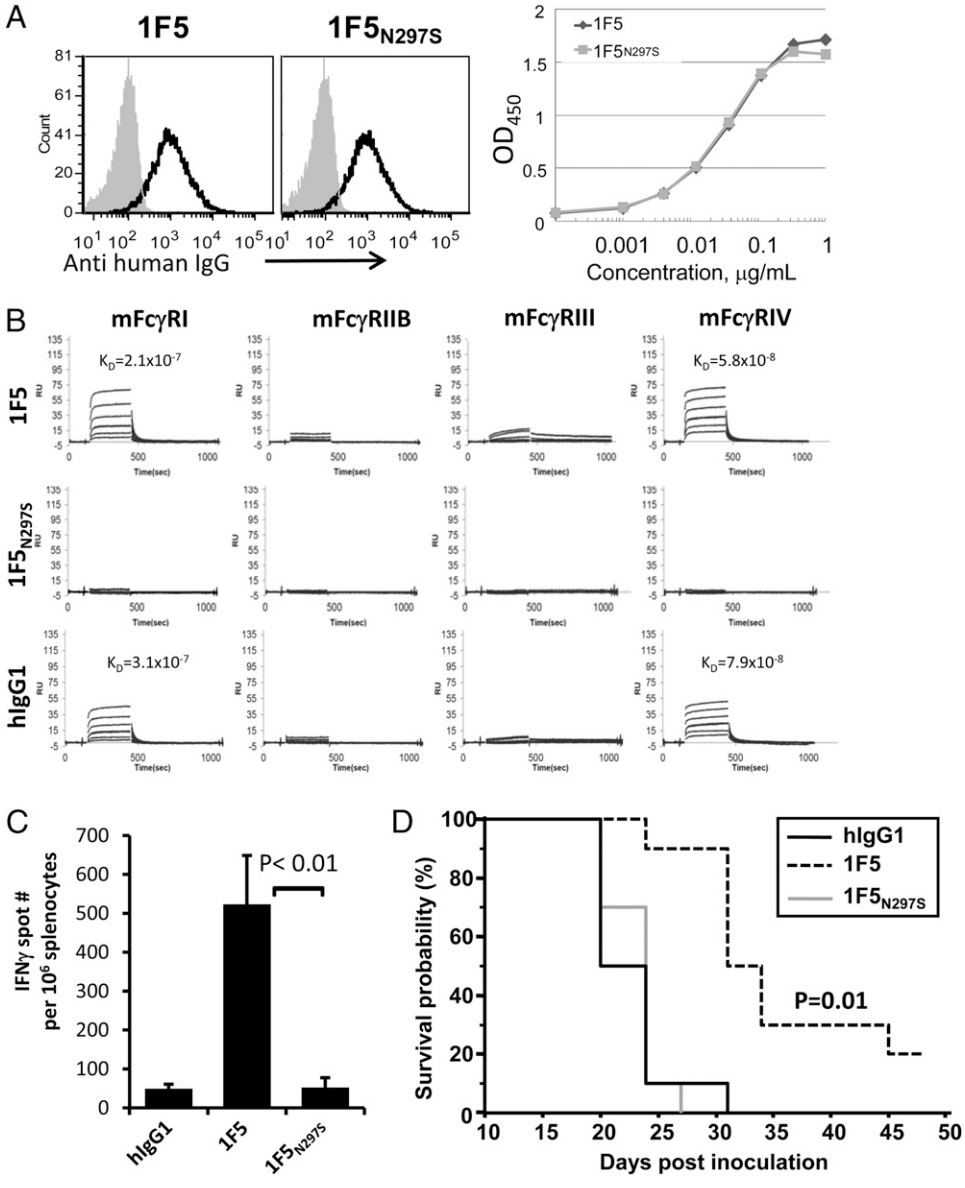

FIGURE 11. FcR engagement is required for in vivo activity of 1F5. (**A**) Binding of 1F5 and $1F5_{N297S}$ to $CD27^+$ cells and rCD27. CCRF-CEM cells were stained with 5 μg/ml Ab, followed by goat anti-human IgG Fc-PE. Open graphs represents Ab; filled graph is nonspecific hIgG1 control. ELISA was performed using a microtiter plate coated with hCD27 and detected with goat anti-human IgG Fc-HRP. (**B**) Surface plasmon resonance analysis of 1F5, $1F5_{N297S}$, and hIgG1 binding to recombinant soluble mouse FcγRs. Sensograms are shown in response units (RU) against time (s). Abs were immobilized at 800 RU and soluble murine FcRs passed over at concentrations from 12.5 to 400 nM. Calculated K_D values (M) for interactions with significant binding are shown. (**C**) hCD27-Tg C57BL/6 mice were injected i.p. with 5 mg of OVA and 50 μg of 1F5. Spleens were collected 1 wk later. Data are mean ± SD of IFN-γ ELISPOT numbers/10^6 splenocytes from three mice/group, and results are representative of three independent experiments. (**D**) Kaplan–Meier survival curves of groups of 10 hCD27-Tg C57BL/6 mice inoculated with 10^6 EG7 cells on day 0 and treated with 100 μg of 1F5, $1F5_{N297S}$, or hIgG1 on days 3, 10, and 17. The *p* value shown is for 1F5 versus $1F5_{N297S}$ or hIgG1.

The 1F5 mAb does not cross-react with mCD27 and is ineffective in WT mice; thus, the T cell activation occurred via signaling through hCD27.

Immunization of hCD27-Tg mice with OVA with the concurrent administration of 1F5 significantly enhanced Ag-specific CD8 T cell expansion and effector function (IFN-γ response), demonstrating that 1F5 was able to trigger the costimulatory signals by binding to hCD27 in vivo. This "adjuvant" effect of 1F5 was dependent on Fc–FcγR interactions, as shown by mutating the 1F5 mAb (IgG1) to a form with greatly reduced binding to FcγRs ($1F5_{N297S}$). This finding emphasizes that CD27 stimulation by specific Abs in vivo may be altered by modifying the isotype or affinity of the Fc domain for FcγR family members, as was shown for anti-CD40 agonist Abs (34, 35).

We demonstrated the antitumor activity of 1F5 monotherapy using several syngeneic models commonly investigated for tumor immunotherapy. Importantly, these tumors express little or no CD27, and no direct binding is observed with the 1F5 Ab (Supplemental Fig. 1). 1F5 was effective at dose levels as low as 10 μg (50 μg total dose) in extending the survival of mice challenged systemically with BCL1 lymphoma cells; however, most mice eventually succumbed to the tumor. We only tested the highest dose of 600 μg in the s.c. colon tumor model CT26 and found that the majority of animals survived the tumor challenge if treated early (starting day 3 after tumor challenge), which was characterized by slow tumor growth and eventual complete regression. However, the efficacy was significantly diminished when treatment was delayed (e.g., when 1F5 therapy was started on ∼day 15), suggesting that, under these conditions, there was insufficient time to develop immunity (median survival without treatment was 31 d) and/or the immunosuppressive mechanisms have overcome the antitumor effect. Importantly, the mice that underwent tumor regression from the initial challenge were resistant to a subsequent administration of CT26 tumor cells given 3 mo after initial treatment with 1F5, indicating that a memory response likely had been established. Consistent with this observation we found that eliminating either $CD4^+$ or $CD8^+$ T cells abrogated the antitumor efficacy of 1F5. The observation that $CD4^+$ cells were also critical to 1F5 activity was not necessarily anticipated, but it may well reflect the importance of promoting a strong helper response to potentiate the cytolytic T cell response. In addition, 1F5 may be impacting regulatory T cells, but additional studies will be required to investigate this point.

The 1F5 mAb also induced protective immunity during the treatment of mice bearing EG7 (EL4-OVA) tumors, and this immunity was partially effective against a subsequent challenge with EL4 cells, suggesting that the tumor immunity was induced against shared Ags and not just against OVA. The antitumor response in the EG7 model was not observed when mice were treated with the mutant $1F5_{N297S}$, indicating the requirement for FcγR engagement for in vivo efficacy of 1F5.

Collectively, these data demonstrate that targeting hCD27 with 1F5 in hCD27-Tg mice can induce T cell activation leading to enhanced Ag-specific immunity and durable antitumor efficacy. The requirement for FcγR engagement for the agonist activity of 1F5 in vivo suggests that the activity of 1F5, and presumably other anti-CD27 mAbs, can be manipulated through selection of the Ab isotype or through specific mutations in the Fc domain that influence the binding to specific FcγRs. In a fashion similar to other immunomodulating Abs, 1F5 exhibited potent antitumor activity when administered soon after tumor challenge, as well as when using tumor models that are considered immunogenic; however, the activity was diminished in the case of delayed treatment. It is likely that for the more challenging tumor models, combinations of 1F5 with vaccines or other interventions that help to induce immunity and/or reduce tumor burden will provide greater efficacy; these studies are underway. These data support 1F5 as a promising candidate for clinical investigation. Phase 1 studies with 1F5, under the name CDX-1127, in patients with advanced solid tumors or hematological malignancies are ongoing.

Acknowledgments

We thank Dr. Yan Zhang for contributions to the IHC studies and Jennifer Widger, Crystal Sisson, Kathleen Borrelli, James Boyer, Eric Forsberg, Lauren Gergel, and Sarah Naylor for expert technical assistance.

Disclosures

L.-Z.H., L.J.T., L.V., J.W., A.C., C.D.P., S.M.R., H.M., and T.K. are employees of Celldex Therapeutics and may hold stock or equity interests in the company. A.T. and M.J.G. are coinventors of U.S. Patent 8,481,029 on the development of agonist anti-CD27 Abs. N.P. has no financial conflicts of interest.

References

1. Mellman, I., G. Coukos, and G. Dranoff. 2011. Cancer immunotherapy comes of age. *Nature* 480: 480–489.
2. Wolchok, J. D., A. S. Yang, and J. S. Weber. 2010. Immune regulatory antibodies: are they the next advance? *Cancer J.* 16: 311–317.
3. Hodi, F. S., S. J. O'Day, D. F. McDermott, R. W. Weber, J. A. Sosman, J. B. Haanen, R. Gonzalez, C. Robert, D. Schadendorf, J. C. Hassel, et al. 2010. Improved survival with ipilimumab in patients with metastatic melanoma. *N. Engl. J. Med.* 363: 711–723.
4. Brahmer, J. R., S. S. Tykodi, L. Q. Chow, W. J. Hwu, S. L. Topalian, P. Hwu, C. G. Drake, L. H. Camacho, J. Kauh, K. Odunsi, et al. 2012. Safety and activity of anti-PD-L1 antibody in patients with advanced cancer. *N. Engl. J. Med.* 366: 2455–2465.
5. Topalian, S. L., F. S. Hodi, J. R. Brahmer, S. N. Gettinger, D. C. Smith, D. F. McDermott, J. D. Powderly, R. D. Carvajal, J. A. Sosman, M. B. Atkins, et al. 2012. Safety, activity, and immune correlates of anti-PD-1 antibody in cancer. *N. Engl. J. Med.* 366: 2443–2454.
6. Rüter, J., S. J. Antonia, H. A. Burris, R. D. Huhn, and R. H. Vonderheide. 2010. Immune modulation with weekly dosing of an agonist CD40 antibody in a phase I study of patients with advanced solid tumors. *Cancer Biol. Ther.* 10: 983–993.
7. Vonderheide, R. H., K. T. Flaherty, M. Khalil, M. S. Stumacher, D. L. Bajor, N. A. Hutnick, P. Sullivan, J. J. Mahany, M. Gallagher, A. Kramer, et al. 2007. Clinical activity and immune modulation in cancer patients treated with CP-870,893, a novel CD40 agonist monoclonal antibody. *J. Clin. Oncol.* 25: 876–883.
8. Weinberg, A. D., N. P. Morris, M. Kovacsovics-Bankowski, W. J. Urba, and B. D. Curti. 2011. Science gone translational: the OX40 agonist story. *Immunol. Rev.* 244: 218–231.
9. Ascierto, P. A., E. Simeone, M. Sznol, Y. X. Fu, and I. Melero. 2010. Clinical experiences with anti-CD137 and anti-PD1 therapeutic antibodies. *Semin. Oncol.* 37: 508–516.
10. Watts, T. H. 2005. TNF/TNFR family members in costimulation of T cell responses. *Annu. Rev. Immunol.* 23: 23–68.
11. van Lier, R. A., J. Borst, T. M. Vroom, H. Klein, P. Van Mourik, W. P. Zeijlemaker, and C. J. Melief. 1987. Tissue distribution and biochemical and functional properties of Tp55 (CD27), a novel T cell differentiation antigen. *J. Immunol.* 139: 1589–1596.
12. Vossen, M. T., M. Matmati, K. M. Hertoghs, P. A. Baars, M. R. Gent, G. Leclercq, J. Hamann, T. W. Kuijpers, and R. A. van Lier. 2008. CD27 defines phenotypically and functionally different human NK cell subsets. *J. Immunol.* 180: 3739–3745.
13. Agematsu, K., S. Hokibara, H. Nagumo, and A. Komiyama. 2000. CD27: a memory B-cell marker. *Immunol. Today* 21: 204–206.
14. Hintzen, R. Q., S. M. Lens, K. Lammers, H. Kuiper, M. P. Beckmann, and R. A. van Lier. 1995. Engagement of CD27 with its ligand CD70 provides a second signal for T cell activation. *J. Immunol.* 154: 2612–2623.
15. Hendriks, J., Y. Xiao, and J. Borst. 2003. CD27 promotes survival of activated T cells and complements CD28 in generation and establishment of the effector T cell pool. *J. Exp. Med.* 198: 1369–1380.
16. Bullock, T. N., and H. Yagita. 2005. Induction of CD70 on dendritic cells through CD40 or TLR stimulation contributes to the development of CD8+ T cell responses in the absence of CD4+ T cells. *J. Immunol.* 174: 710–717.
17. Taraban, V. Y., T. F. Rowley, D. F. Tough, and A. Al-Shamkhani. 2006. Requirement for CD70 in CD4+ Th cell-dependent and innate receptor-mediated CD8+ T cell priming. *J. Immunol.* 177: 2969–2975.
18. Yang, F. C., K. Agematsu, T. Nakazawa, T. Mori, S. Ito, T. Kobata, C. Morimoto, and A. Komiyama. 1996. CD27/CD70 interaction directly induces natural killer cell killing activity. *Immunology* 88: 289–293.
19. Hintzen, R. Q., S. M. Lens, M. P. Beckmann, R. G. Goodwin, D. Lynch, and R. A. van Lier. 1994. Characterization of the human CD27 ligand, a novel member of the TNF gene family. *J. Immunol.* 152: 1762–1773.

20. Tesselaar, K., L. A. Gravestein, G. M. van Schijndel, J. Borst, and R. A. van Lier. 1997. Characterization of murine CD70, the ligand of the TNF receptor family member CD27. *J. Immunol.* 159: 4959–4965.
21. Couderc, B., L. Zitvogel, V. Douin-Echinard, L. Djennane, H. Tahara, G. Favre, M. T. Lotze, and P. D. Robbins. 1998. Enhancement of antitumor immunity by expression of CD70 (CD27 ligand) or CD154 (CD40 ligand) costimulatory molecules in tumor cells. *Cancer Gene Ther.* 5: 163–175.
22. Nieland, J. D., Y. F. Graus, Y. E. Dortmans, B. L. Kremers, and A. M. Kruisbeek. 1998. CD40 and CD70 co-stimulate a potent in vivo antitumor T cell response. *J. Immunother.* 21: 225–236.
23. Arens, R., K. Schepers, M. A. Nolte, M. F. van Oosterwijk, R. A. van Lier, T. N. Schumacher, and M. H. van Oers. 2004. Tumor rejection induced by CD70-mediated quantitative and qualitative effects on effector CD8+ T cell formation. *J. Exp. Med.* 199: 1595–1605.
24. Rowley, T. F., and A. Al-Shamkhani. 2004. Stimulation by soluble CD70 promotes strong primary and secondary CD8+ cytotoxic T cell responses in vivo. *J. Immunol.* 172: 6039–6046.
25. Keller, A. M., A. Schildknecht, Y. Xiao, M. van den Broek, and J. Borst. 2008. Expression of costimulatory ligand CD70 on steady-state dendritic cells breaks CD8+ T cell tolerance and permits effective immunity. *Immunity* 29: 934–946.
26. van Gisbergen, K. P., P. L. Klarenbeek, N. A. Kragten, P. P. Unger, M. B. Nieuwenhuis, F. M. Wensveen, A. ten Brinke, P. P. Tak, E. Eldering, M. A. Nolte, and R. A. van Lier. 2011. The costimulatory molecule CD27 maintains clonally diverse CD8(+) T cell responses of low antigen affinity to protect against viral variants. *Immunity* 35: 97–108.
27. French, R. R., V. Y. Taraban, G. R. Crowther, T. F. Rowley, J. C. Gray, P. W. Johnson, A. L. Tutt, A. Al-Shamkhani, and M. J. Glennie. 2007. Eradication of lymphoma by CD8 T cells following anti-CD40 monoclonal antibody therapy is critically dependent on CD27 costimulation. *Blood* 109: 4810–4815.
28. Sakanishi, T., and H. Yagita. 2010. Anti-tumor effects of depleting and non-depleting anti-CD27 monoclonal antibodies in immune-competent mice. *Biochem. Biophys. Res. Commun.* 393: 829–835.
29. Roberts, D. J., N. A. Franklin, L. M. Kingeter, H. Yagita, A. L. Tutt, M. J. Glennie, and T. N. Bullock. 2010. Control of established melanoma by CD27 stimulation is associated with enhanced effector function and persistence, and reduced PD-1 expression of tumor infiltrating CD8(+) T cells. *J. Immunother.* 33: 769–779.
30. Vitale, L. A., L. Z. He, L. J. Thomas, J. Widger, J. Weidlick, A. Crocker, T. O'Neill, J. Storey, M. J. Glennie, D. M. Grote, et al. 2012. Development of a human monoclonal antibody for potential therapy of CD27-expressing lymphoma and leukemia. *Clin. Cancer Res.* 18: 3812–3821.
31. Gravestein, L. A., J. D. Nieland, A. M. Kruisbeek, and J. Borst. 1995. Novel mAbs reveal potent co-stimulatory activity of murine CD27. *Int. Immunol.* 7: 551–557.
32. Xiao, Y., J. Hendriks, P. Langerak, H. Jacobs, and J. Borst. 2004. CD27 is acquired by primed B cells at the centroblast stage and promotes germinal center formation. *J. Immunol.* 172: 7432–7441.
33. Tao, M. H., and S. L. Morrison. 1989. Studies of aglycosylated chimeric mouse-human IgG. Role of carbohydrate in the structure and effector functions mediated by the human IgG constant region. *J. Immunol.* 143: 2595–2601
34. Li, F., and J. V. Ravetch. 2011. Inhibitory Fcγ receptor engagement drives adjuvant and anti-tumor activities of agonistic CD40 antibodies. *Science* 333: 1030–1034.
35. White, A. L., H. T. Chan, A. Roghanian, R. R. French, C. I. Mockridge, A. L. Tutt, S. V. Dixon, D. Ajona, J. S. Verbeek, A. Al-Shamkhani, et al. 2011. Interaction with FcγRIIB is critical for the agonistic activity of anti-CD40 monoclonal antibody. *J. Immunol.* 187: 1754–1763.

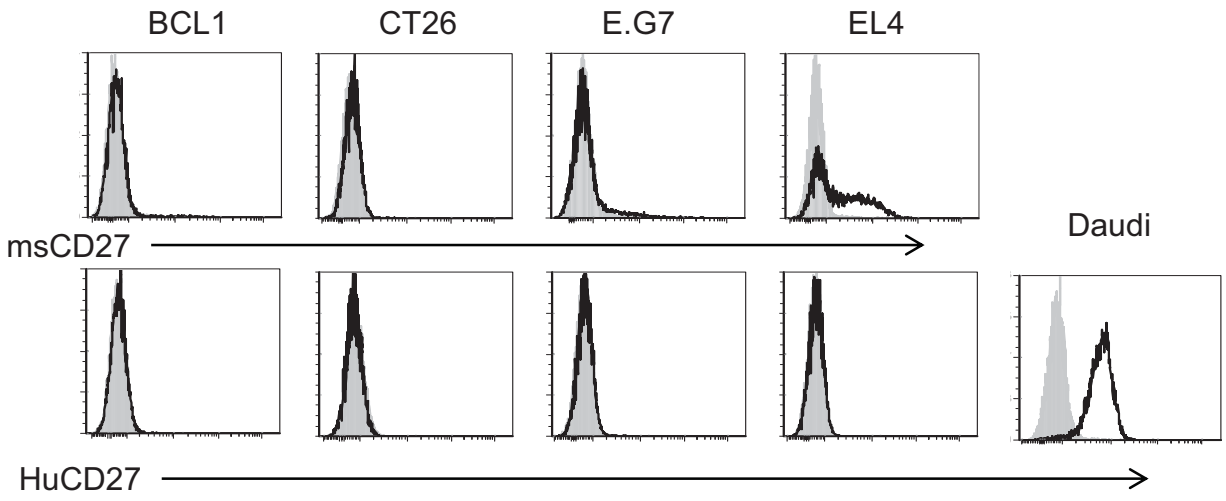

Supplemental Figure 1. 1F5 does not bind to murine tumor cell lines. Mouse tumor cells (BCL1, CT26, E.G7, and EL4) used for tumor challenge studies were stained with rabbit anti-mCD27, 1F5 (anti-hCD27) or isotype controls (shaded histogram) and analyzed by flow cytometry. The human lymphoblastoma Daudi cells were included for a positive control for 1F5 binding.